Numerical solution of steady Euler equations in streamline-aligned orthogonal coordinates.

A.M. Latypov

Department of Mathematics and Statistics
and Fluid Dynamics Research Institute,
University of Windsor, 401 Sunset Ave.,
Windsor, Ontario, Canada N9B 3P4.
Internet email: latypov@server.uwindsor.ca

Abstract: Formulating the governing equations of fluid motion in streamline coordinates allows one to avoid difficulties associated with grid generation and to solve problems of inverse design or problems with free boundaries.

The governing equations for steady inviscid two-dimensional gas motion are written in an orthogonal system of independent coordinates consisting of the streamfunction and its orthogonal complimentary function. The result is a system of differential conservation laws, expressing conservation of mass, momentum and energy. The conservative finite volume approximation of these equations can be used to calculate flows with strong shocks. For the case of potential velocity vector field, two different simplified formulations of the governing equations are derived.

In order to compute purely supersonic flows, a conservative hybrid grid-characteristic scheme has been developed. To calculate transonic potential flows, two iterative algorithms have been implemented.

The calculated examples include supersonic flow over a wedge, supersonic flow in an axisymmetric channel and in a jet emerging from this channel, and transonic flows in a nozzle and an axisymmetric bumpy channel.

1 Introduction.

There are several advantages in formulating the governing equations of steady gas motion in a system of independent coordinates aligned with streamlines.

Von Mises [1] used the streamfunction as one of the independent coordinates in boundary layer studies. The second independent coordinate was chosen to be the transverse Cartesian coordinate to the flow direction. Stanitz developed a modification of von Mises approach in [2] and [3] in order to solve inverse design problems of potential gas dynamics. The essence of Stanitz's modification was that a velocity vector potential was used as the second independent coordinate instead of the transverse Cartesian coordinate.

A related and more general approach was suggested by Martin in inviscid gas dynamics [4] as well as in viscous incompressible fluid dynamics [5].

During the last 15 years, a number of techniques, based upon the "streamfunction-as-a-coordinate" (SFC) ideology, have been used in Computational Fluid Dynamics (CFD). The latest review of these works as well as a bibliography can be found in [6].

One of the attractive advantages provided by the SFC ideology in CFD applications is that it permits computation of the parameters of the flow without prior grid generation in the computational domain. More exactly, the governing equations play a double role of both the equations describing the motion of the media and the grid generation equations. As a result of this, both the computational time and the memory requirements can be reduced. Furthermore, the resulting streamline-aligned computational grid naturally conforms to the boundaries of the physical domain. These features are utilized in most of the works dealing with the SFC method in CFD (see [6]–[43]).

Other applications of CFD, in which the SFC concept has been found to be useful, include the class of problems with initially unknown shape of a boundary segment. Typical problems belonging to this class are ones with free or elastic boundaries, problems involving inverse design of aerodynamic shapes for given distribution of some physical quantities (eg, pressure) along a segment of the boundary, or problems involving the optimal design of the shape, which provides the maximum or minimum to some integral functional, calculated from the solution (eg, minimization of a drag force, or maximization of a lift force acting on an airfoil).

The common feature of problems falling into this category is that the shape of at least a part of the boundary is not given, but rather needs to be determined as a result of the solution procedure. As a consequence, the use of conventional iterative approaches requires adjusting the computational grid to the geometry of the domain at each iteration. Since the typical domain in this class of problems is bounded by streamlines, the SFC technique makes it possible to avoid the costly procedure of grid recalculation.

This advantage has been exploited in a number of works. Applications of the SFC concept to airfoil, turbomachinery and nozzle inverse design problems can be found in [2, 3, 15, 16, 17, 24, 25, 29]. A problem in which the shape of the nozzle wall is prescribed everywhere but in the vicinity of the nozzle's throat is considered in [42]. The shape of the wall near the throat is designed so that the distribution of pressure along this part of the wall remains smooth.

The SFC technique has been successfully applied to the numerical solution of free boundary problems involving jets in [26, 32, 33, 34].

Among the areas of application mentioned above, problems with elastic boundaries and problems of optimal design of aerodynamic shapes remain the areas in which the SFC technique's advantages have not been widely utilized thus far.

Although the SFC concept has mainly been used in theoretical fluid dynamics and CFD due to its advantages in the fields mentioned above, there exist a number of works extending this methodology to other applications. In [35, 36, 37] streamline independent coordinates have been applied to the study of turbulence and chaos occurring in a fluid flow. In [18, 19] properties of a flow in porous media were investigated using the von Mises coordinates. This coordinate transformation has also been applied to two-phase fluid flow in [10]. In the latter case, one needs to consider two streamfunctions, each corresponding to one of the phases existing in the flow. In [38] a streamline-aligned coordinate transformation was used in order to obtain a simplified form of the Navier-Stokes equations. This simplification (called the "parabolized" Navier-Stokes equations) is based on neglecting some of the second order spatial derivatives in order to make the steady-state equations elliptic only within the boundary layer and parabolic elsewhere. This feature simplifies the numerical solution of the resulting system, while giving better approximation to the original Navier-Stokes equations than obtained from the boundary layer theory. As an order

of magnitude comparison shows, the terms to be neglected are to be chosen from those containing the second order derivatives in the direction of the flow. Writing the governing equations in a streamline-aligned coordinate system simplifies the selection of terms to be neglected.

An essential feature of the SFC technique is the choice of the independent coordinate or coordinates which compliment the streamfunction to produce the nondegenerate system of independent coordinates. It is well known that one of the major limitations of the original von Mises approach [1] is that the resulting system of coordinates degenerates at the locations where the velocity vector is normal to the axis of the transverse Cartesian coordinate. This situation is typical for the flow in the vicinity of the leading edge of an airfoil. This limits applicability of the von Mises approach to cases where one can expect in advance that the flow direction will not change significantly over the flow domain.

A number of modifications to the von Mises coordinates have been tried. A discussion and references on this issue can be found in [6]. Out of the most recent approaches, not covered in the above-cited review, one should mention the technique developed in [21, 22, 23], in which it is advocated to use the Lagrangian time as a complimentary independent coordinate to two streamfunctions in three-dimensional steady gas flow.

In the current work we consider a streamline–based transformation which generates an orthogonal streamwise coordinate system. Such a coordinate system, generated by streamfunction and velocity vector potential for the solution of design problems in inviscid compressible potential flows, was suggested in [2, 3]. Later, this approach was generalized to nonpotential flows by a number of authors (eg, [30, 31, 32, 43]).

The orthogonality of this system ensures that, even in the case of a flow region with complex geometry, the coordinate transformation does not degenerate. A further advantage of the formulation used in the current work is that it is expressed as a system of "physically consistent" conservation laws and, as a consequence, it may be used to calculate flows with shocks.

In Section 2, the streamline-aligned orthogonal coordinates are introduced and the Euler equations are formulated in this coordinate system. The case of potential flow is also considered and two different full–potential–equivalent formulations are proposed. Then, the characteristics and compatibility conditions for the governing system are derived, and the boundary conditions are formulated and discussed.

In Section 3, a conservative hybrid grid-characteristics scheme for supersonic flow calculations is constructed.

In Section 4 and Section 5, the numerical algorithms to solve the transonic full–potential–equivalent equations are given.

Finally, in Section 6, sample computations are performed using the constructed numerical techniques.

2 Governing Equations in Streamline Independent Coordinates

2.1 Streamline Independent Coordinates

Consider the system of steady two-dimensional Euler equations in Cartesian coordinates (x, y):

$$\frac{\partial w}{\partial x} + \frac{\partial f}{\partial y} = \nu h, \tag{1}$$

where

$$w = \begin{bmatrix} y^\nu \rho u \\ y^\nu (p + \rho u^2) \\ y^\nu \rho uv \\ y^\nu \rho uD \\ Cv \end{bmatrix}, \quad f = \begin{bmatrix} y^\nu \rho v \\ y^\nu \rho uv \\ y^\nu (p + \rho v^2) \\ y^\nu \rho vD \\ -Cu \end{bmatrix}, \quad h = \begin{bmatrix} 0 \\ 0 \\ p \\ 0 \\ 0 \end{bmatrix},$$

and

$$\begin{array}{lcll} D & = & \frac{q^2}{2} + e + \frac{p}{\rho} & - \text{full enthalpy,} \\ q^2 & = & u^2 + v^2, & \\ e & = & \frac{1}{\gamma - 1} \frac{p}{\rho} & - \text{internal energy of a perfect gas} \\ C & & & - \text{the unknown function.} \end{array}$$

$$\nu = \begin{cases} 0, & \text{for plane flows,} \\ 1, & \text{for axisymmetric flows.} \end{cases}$$

The equations (1.1)– (1.4) express the conservation of mass, two components of momentum and energy respectively. Here and in the following we use the notations like (1.i) to refer to the i-th equation of the system (1).

Consider two differential relations :

$$d\varphi = C(udx + vdy), \tag{2}$$

$$d\psi = B(\psi) y^\nu \rho (udy - vdx), \tag{3}$$

where $B(\psi)$ is a given positive function, which will be used to refine the mesh. It should be noted that the right-hand sides of both (2) and (3) are the full differentials because of the equations (1.1) and (1.5) respectively. It should also be emphasised that (1.5) shows that the new unknown function C is an integrating factor, which makes it possible to introduce φ in the general case of vortical flow. Therefore, (2) and (3) define a pair of functions:

$$\begin{array}{rcl} \varphi & = & \varphi(x, y) \\ \psi & = & \psi(x, y). \end{array}$$

The value of each of these functions is known up to one arbitrary constant.

It follows from (2) and (3) that:

$$v \cdot \nabla \psi = 0, \tag{4}$$

$$\nabla \psi \cdot \nabla \varphi = 0, \tag{5}$$

where v is a velocity vector. In other words, contours of ψ are aligned along the direction of a velocity vector field, while contours of φ are perpendicular to this direction. The pair of functions φ and ψ will be further referred to as *streamline coordinates* or *streamline variables*.

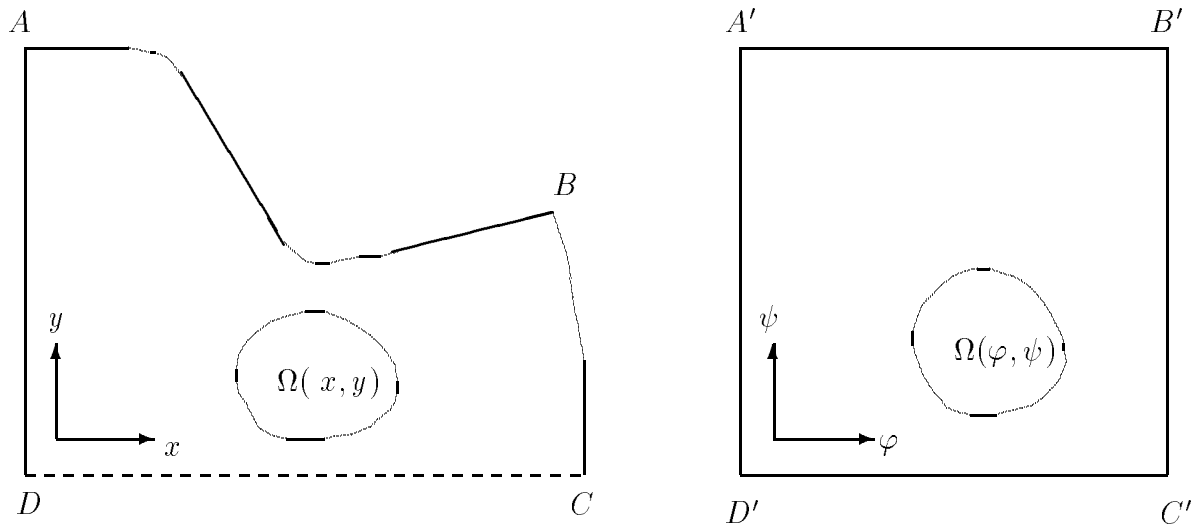

Figure 1: Original and mapped domains.

2.2 Derivation of the Governing Equations in Streamline–Aligned Orthogonal Coordinates

The change of independent variables from x and y to φ and ψ in (1) may be done as in [43] – that is using (2) and (3) and the chain rule:

$$\begin{aligned}
\frac{\partial}{\partial x} &= \frac{\partial \varphi}{\partial x}\frac{\partial}{\partial \varphi} + \frac{\partial \psi}{\partial x}\frac{\partial}{\partial \psi} \\
&= Cu\frac{\partial}{\partial \varphi} - B(\psi)y^{\nu}\rho v\frac{\partial}{\partial \psi} \\
\frac{\partial}{\partial y} &= \frac{\partial \varphi}{\partial y}\frac{\partial}{\partial \varphi} + \frac{\partial \psi}{\partial y}\frac{\partial}{\partial \psi} \\
&= Cv\frac{\partial}{\partial \varphi} + B(\psi)y^{\nu}\rho u\frac{\partial}{\partial \psi}
\end{aligned}$$

In the current work, however, the same is done using the change of independent variables in the system of integral conservation laws, corresponding to (1). Apart from simplifying the algebra, this would enable us to obtain the governing system in φ - ψ coordinates, written as a system of conservation laws.

Consider a gas flow in the domain $ABCD$ (Fig. 1). We assume that the boundary AB is a solid wall, CD is either a solid wall or a plane/axis of symmetry, AD – the "inlet" and BC – the "outlet" are both orthogonal to the local direction of v.

It is well known that the system of Euler equations may not have a solution in a classical sense even if the boundary data are smooth enough. In order to take into account non–smooth flows (that is those with shocks or contact discontinuities), one should consider the concept of a weak solution.

Consider an arbitrary subdomain $\Omega(x,y)$ of $ABCD$. Integrating (1) over $\Omega(x,y)$ and applying Gauss' theorem, one obtains:

$$\oint_{\partial\Omega(x,y)} w dy - f dx = \nu \int\int_{\Omega(x,y)} h dx dy \tag{6}$$

We say that (1) has *a weak solution in $ABCD$* if (6) is valid for any subdomain $\Omega(x,y)$.

After a transformation to the coordinates φ - ψ , $ABCD$ becomes a rectangle $A'B'C'D'$, while $\Omega(x,y)$ maps into $\Omega(\varphi,\psi)$ (Fig. 1).

To define a weak solution in φ - ψ plane, which is consistent with (6), one should express dx, dy and $dxdy$ from (6) in terms of $d\varphi$, $d\psi$ and $d\varphi d\psi$. It follows from (2) and (3) that:

$$\begin{aligned} dy &= uJ_1 d\psi + vJ_2 d\varphi, && (7)\\ dx &= -vJ_1 d\psi + uJ_2 d\varphi, && (8)\\ dxdy &= q^2 J_1 J_2 d\psi d\varphi, && (9) \end{aligned}$$

where,

$$\begin{aligned} J_1 &= \frac{1}{B(\psi) y^\nu \rho q^2},\\ J_2 &= \frac{1}{Cq^2}. \end{aligned}$$

However, the substitution of (7)–(9) into (6) shows that the right–hand sides of the relations (6.1) and (6.5) become identically zero and therefore the corresponding relations in the φ - ψ plane are both equivalences. The reason for this is that the transformation to the φ - ψ variables is only possible when the consistency relations (1.1) and (1.5) are hold. In other words, the very existence of the variables φ - ψ as the unique–valued functions of x and y (which is assumed before doing the change of variables in (6)) implies that the equations (1.1) and (1.5) (together with the relations (6.1) and (6.5), corresponding to them) are valid. As a consequence, (6.1) and (6.5) are automatically satisfied in φ - ψ plane.

At the same time, the right-hand sides of (7) and (8) must be full differentials, in order for these relations to be consistent. This gives the following conditions:

$$\oint_{\partial\Omega(\varphi,\psi)} vJ_2 d\varphi + uJ_1 d\psi = 0, \qquad (10)$$

$$\oint_{\partial\Omega(\varphi,\psi)} uJ_2 d\varphi - vJ_1 d\psi = 0, \qquad (11)$$

for any domain $\Omega(\varphi,\psi)$ from $A'B'C'D'$.

Adding (10) and (11) to (6.2)–(6.4), rewritten in the φ - ψ plane, one obtains the following system of integral conservation laws:

$$\oint_{\partial\Omega(\varphi,\psi)} W d\psi - F d\varphi = \nu \int\int_{\Omega(\varphi,\psi)} H d\varphi d\psi, \qquad (12)$$

where

$$W = \begin{bmatrix} uJ_1 \\ vJ_1 \\ u(p+\rho q^2) y^\nu J_1 \\ v(p+\rho q^2) y^\nu J_1 \\ D \end{bmatrix}, \quad F = \begin{bmatrix} -vJ_2 \\ uJ_2 \\ -vpy^\nu J_2 \\ upy^\nu J_2 \\ 0 \end{bmatrix}, \quad H = \begin{bmatrix} 0 \\ 0 \\ 0 \\ pq^2 J_1 J_2 \\ 0 \end{bmatrix},$$

For smooth flows (12) is equivalent to :

$$\frac{\partial W}{\partial \varphi} + \frac{\partial F}{\partial \psi} = \nu H, \tag{13}$$

which is the governing system of equations written in streamline–aligned orthogonal variables. In the following, we assume that the fluxes W and F in (13) are functions of the vector of primitive variables U, which in this work is chosen to be $U = (z, \theta, C, S, D)^T$, where:

$$\begin{array}{lll} z & = M^2 & \text{– squared Mach number,} \\ \theta & = \arctan(\frac{v}{u}) & \text{– velocity vector argument,} \\ S & = \frac{p}{\rho^\kappa} & \text{– entropy function,} \\ \kappa & & \text{– specific heat ratio.} \end{array}$$

Similar to the definition of the weak solution to (1), we say that (13) has *a weak solution in* $A'B'C'D'$, if (12) is valid for any subdomain $\Omega(\varphi, \psi)$.

2.3 Proof of the Governing System Formulation in Streamline Coordinates

In Section 2.2 the consistency conditions (10) and (11) were added to the system (13) as a substitute for the continuity equation (1.1) and the equation (1.5) which are automatically satisfied in the φ - ψ plane. Unlike (1.1) and (1.5), the equations (10) and (11) have no direct physical meaning, and in order to justify this substitution we give in this Section a more formal proof.

Namely, the following Proposition is proven.

Proposition 1 *Assuming the following is true:*

1. *$U = U(\varphi, \psi)$ is a weak solution of (13) in $A'B'C'D'$;*
2. *The functions $x = x(\varphi, \psi)$ and $y = y(\varphi, \psi)$ are defined on $A'B'C'D'$ as follows:*

$$x = x_0 + \int_{(\varphi_0, \psi_0)}^{(\varphi, \psi)} -v J_1 d\psi + u J_2 d\varphi, \tag{14}$$

$$y = y_0 + \int_{(\varphi_0, \psi_0)}^{(\varphi, \psi)} u J_1 d\psi + v J_2 d\varphi, \tag{15}$$

where x_0 and y_0 are the values of x and y at the point (φ_0, ψ_0), which may be chosen arbitrarily, and

3. *(14) and (15) map $A'B'C'D'$ to a domain $ABCD$ in the x–y plane and this mapping can be globally inverted:*

$$A'B'C'D' \quad \begin{array}{c} x=x(\varphi,\psi), \\ y=y(\varphi,\psi) \\ \longleftrightarrow \\ \varphi=\varphi(x,y) \\ \psi=\psi(x,y) \end{array} \quad ABCD \tag{16}$$

Then, $\tilde{U}(x,y) = U(\varphi(x,y), \psi(x,y))$ is a weak solution of (1).

Remark. Because of the relations (12.1) and (12.2) from the definition of the weak solution in the φ-ψ plane, the values of the contour integrals (14) and (15) are path independent.

Proof of the Proposition 1. To prove the proposition we need to prove the validity of (6) for all $\Omega(x,y) \subset ABCD$.

Let $\Omega(\varphi,\psi)$ be the image of $\Omega(x,y)$ under the mapping (16).

We first notice that (12.3)– (12.5) from the definition of a weak solution in the φ - ψ plane have been derived in Section 2.2 from the relations (6.2)–(6.4) respectively, using the change of variables (7)–(9). Starting from (12.3)– (12.5) (which are valid by the definition of a weak solution in the φ - ψ plane) and proceeding backwards, one can easily obtain (6.2)–(6.4).

To prove (6.1) we write :

$$\oint_{\partial\Omega(x,y)} y^\nu \rho u dy - y^\nu \rho v dx =$$
$$\oint_{\partial\Omega(\varphi,\psi)} y^\nu \rho u (u J_1 d\psi + v J_2 d\varphi) - y^\nu \rho v (-v J_1 d\psi + u J_2 d\varphi) =$$
$$\oint_{\partial\Omega(\varphi,\psi)} 0 \; d\varphi + \frac{d\psi}{B(\psi)} \equiv 0.$$

In a similar way we can write for (6.5):

$$\oint_{\partial\Omega(x,y)} C v dy - C u dx =$$
$$\oint_{\partial\Omega(\varphi,\psi)} C v (u J_1 d\psi + v J_2 d\varphi) - C u (-v J_1 d\psi + u J_2 d\varphi) =$$
$$\oint_{\partial\Omega(\varphi,\psi)} d\,\varphi + 0 d\psi \equiv 0.$$

This completes the proof of the Proposition 1.

Remark. It is known [44] that for discontinuous flows (6) leads to a system of algebraic relations for values of the gas parameters along both sides of the discontinuity:

$$[w](\frac{dy}{dx})_{disc.} - [f] = 0, \tag{17}$$

where,

$(\frac{dy}{dx})_{disc.}$ – local slope of the discontinuity,

$[a]$ – denotes jump of the quantity a.

It follows from Proposition 1, that the weak solution of (12) mapped onto the x-y plane satisfies (17). Consequently, the conservative approximation of the equation (13) may be used for the calculation of flows with shocks.

We also mention here, without proof, that in addition to shock or contact discontinuity conditions for the gas parameters [44], the unknown function C satisfies the relations:

$$\begin{aligned} [C] &= 0 \qquad\qquad \text{across a shock,} \\ [Cq] &= 0 \quad \text{across a contact discontinuity.} \end{aligned}$$

2.4 The Governing System for Potential Flows

The assumptions that the velocity vector field is potential (irrotational) and that the flow is isentropic ($S \equiv const$) and isenthalpic ($D \equiv const$) are well established in modelling of compressible flows. The reasons for this is that, under these assumptions, the equations of momentum and energy follow from the continuity equation and the condition that the velocity vector has a potential. Also, in this case, the governing system may be reduced to just one second–order equation for the velocity vector potential. However, on the other hand, these assumptions are not valid if the flow contains strong curved shocks.

Following [44], we can write the governing system in Cartesian coordinates as:

$$\frac{\partial w^{(p)}}{\partial x} + \frac{\partial f^{(p)}}{\partial y} = 0, \tag{18}$$

where,

$$w^{(p)} = \begin{bmatrix} y^\nu \rho u \\ v \end{bmatrix}, \quad f^{(p)} = \begin{bmatrix} y^\nu \rho v \\ -u \end{bmatrix},$$

The streamline coordinates are again introduced through the relations (2) and (3). But, as it follows from (18.2) and these relations , there is no longer need to resort to the unknown C (an integrating factor). We may set C equal to any positive function of φ:

$$C = C(\varphi).$$

As the function $B(\psi)$, $C(\varphi)$ serves to control the refinement of the mesh in x–y coordinates.

The governing system in φ–ψ coordinates then reduces to:

$$\frac{\partial W^{(p)}}{\partial \varphi} + \frac{\partial F^{(p)}}{\partial \psi} = 0, \tag{19}$$

where,

$$W^{(p)} = \begin{bmatrix} uJ_1 \\ vJ_1 \end{bmatrix}, \quad F^{(p)} = \begin{bmatrix} -vJ_2 \\ uJ_2 \end{bmatrix},$$

The vector of primitive variables in this case is chosen to be $U^{(p)} = (z, \theta)^T$.

In the following, we consider two full–potential–equivalent formulations of the governing system. In each of these cases the result is a set of second order equations, each of which can be solved numerically, using computational methods which have been developed for the full–potential equation.

2.4.1 Reduction of the governing equations to a single second order equation

It follows from (7) that:

$$\frac{u}{\rho q^2} = B(\psi) y^\nu \frac{\partial y}{\partial \psi}, \tag{20}$$

$$\frac{v}{q^2} = C(\varphi) \frac{\partial y}{\partial \varphi}. \tag{21}$$

Substituting these relations into the condition for the right–hand side of (8) to be a full differential, we obtain:

$$\frac{\partial}{\partial \varphi}\Big(f \frac{\partial y}{\partial \varphi}\Big) + \frac{\partial}{\partial \psi}\Big(\frac{1}{f} \frac{\partial y}{\partial \psi}\Big) = 0, \tag{22}$$

where,

$$f = \frac{J_1}{J_2} = \frac{C(\varphi)}{B(\psi) y^\nu \rho}. \tag{23}$$

Note that equation (22) is (19.2), written in terms of y and its derivatives, and that (19.1) is also satisfied because of the relations (20)–(21). Therefore, (22) can be taken as a governing equation in place of the system (19).

If the function $y = y(\varphi, \psi)$ is given, the primitive variables z and θ can be calculated from (20)–(21), because in an isentropic and isenthalpic flow ρ and q are both known functions of z, and $u = q \cos\theta$ and $v = q \sin\theta$.

However:

$$\frac{\partial\left(\frac{u}{\rho q^2}, \frac{v}{q^2}\right)}{\partial(z, \theta)} = \frac{1 - z\cos^2\theta}{z(2 + (\kappa - 1)z)\rho q^2}$$

This means that for transonic flows containing the so–called limiting lines on which $z \cos^2\theta = 1$, the set of equations (20) and (21) cannot be uniquely resolved with respect to z and θ. To chose the correct root in (20) and (21) one more differential equation has to be applied in the transonic regions of flow [41].

2.4.2 System of two second order equations

In this section, an alternative formulation which makes it possible to avoid the problem of nonuniqueness of the solution to the system (20) and (21) is derived.

Using (7) and (8), the fluxes W and F can be written in terms of the partial derivatives of the functions $x = x(\varphi, \psi)$ and $y = y(\varphi, \psi)$:

$$W^{(p)} = \begin{bmatrix} f \frac{\partial x}{\partial \varphi} \\ f \frac{\partial y}{\partial \varphi} \end{bmatrix}, \quad F^{(p)} = \begin{bmatrix} \frac{1}{f} \frac{\partial x}{\partial \psi} \\ \frac{1}{f} \frac{\partial y}{\partial \psi} \end{bmatrix},$$

where, again f is given by (23), but z and θ are to be determined from :

$$\frac{u}{q^2} = C(\varphi)\frac{\partial x}{\partial \varphi}, \tag{24}$$

$$\frac{v}{q^2} = C(\varphi)\frac{\partial y}{\partial \varphi}. \tag{25}$$

Unlike the Jacobian of the system (20) and (21), the Jacobian of (24) and (25) does not become zero, and, consequently, the latter system can be resolved with respect to z and θ in a unique way.

The set of equations (19) then becomes a system of two coupled second order equations for x and y.

2.5 Characteristics and Compatibility Conditions for the Governing System

In this section we derive the characteristic directions and the compatibility conditions along these characteristics for the governing system (13) in the case of plane geometry ($\nu = 0$). [1]

Equation (13) can be rewritten as:

$$A^{(\varphi)}\frac{\partial U}{\partial \varphi} + A^{(\psi)}\frac{\partial U}{\partial \psi} = 0, \tag{26}$$

where U is a vector of primitive variables, and

$$A^{(\varphi)} = \frac{\partial W}{\partial U} = \begin{pmatrix} (z-1)g(z)W^{(1)} & -W^{(2)} & 0 & W^{(1)}/(\gamma S) & -(\kappa+1)W^{(1)}/(2\gamma D) \\ (z-1)g(z)W^{(2)} & W^{(1)} & 0 & W^{(2)}/(\gamma S) & -(\kappa+1)W^{(2)}/(2\gamma D) \\ (z-1)g(z)pW^{(1)} & -W^{(4)} & 0 & 0 & -W^{(3)}/(2D) \\ (z-1)g(z)pW^{(2)} & W^{(3)} & 0 & 0 & -W^{(4)}/(2D) \\ 0 & 0 & 0 & 0 & 1 \end{pmatrix}$$

$$A^{(\psi)} = \frac{\partial F}{\partial U} = \begin{pmatrix} -g(z)F^{(1)} & -F^{(2)} & -F^{(1)}/C & 0 & -F^{(1)}/(2D) \\ -g(z)F^{(2)} & F^{(1)} & -F^{(2)}/C & 0 & -F^{(2)}/(2D) \\ -(1+\kappa z)g(z)F^{(3)} & -F^{(4)} & -F^{(3)}/C & -F^{(3)}/(\gamma S) & -(\kappa+1)F^{(3)}/(2\gamma D) \\ -(1+\kappa z)g(z)F^{(4)} & F^{(3)} & -F^{(4)}/C & -F^{(4)}/(\gamma S) & -(\kappa+1)F^{(4)}/(2\gamma D) \\ 0 & 0 & 0 & 0 & 0 \end{pmatrix}$$

Here, $W^{(i)}$ and $F^{(i)}$ denote the i–th components of the vectors W and F respectively, and,

$$\gamma = \kappa - 1,$$

$$g(z) = \frac{1}{z(2+\gamma z)}.$$

[1] See the Remark on page 13 for the details concerning the case $\nu = 1$.

Following [44], consider the eigenvector problem (*the characteristic equation*) :

$$\boldsymbol{\omega}_i^T(\xi_i^{(\varphi)}A^{(\varphi)} + \xi_i^{(\psi)}A^{(\psi)}) = 0^T, \tag{27}$$

where $\xi_i^{(\varphi)}$ and $\xi_i^{(\psi)}$ are the eigenvalues, and $\boldsymbol{\omega}_i$ are the corresponding eigenvectors.
The characteristics directions are then given by

$$\xi_i^{(\varphi)}d\varphi + \xi_i^{(\psi)}d\psi = 0. \tag{28}$$

To find the compatibility conditions along these characteristics we need to multiply (26) by rows $\boldsymbol{\omega}_i^T$, while also taking into account (27).
The described procedure yields the following:

1. *Contact characteristics* ($\mathcal{C}_0$) :

$$\begin{aligned}
\xi_1^{(\varphi)} &= \xi_2^{(\varphi)} = 0, \\
\xi_{1,2}^{(\psi)} &\quad \text{may be chosen arbitrarily}, \\
\boldsymbol{\omega}_1^T &= (0,0,0,0,1), \\
\boldsymbol{\omega}_2^T &= (-F^{(4)}, F^{(3)}, F^{(2)}, -F^{(1)}, 0).
\end{aligned}$$

The compatibility conditions are:

$$\begin{aligned}
\frac{\partial D}{\partial \varphi} &= 0, \\
\frac{\partial S}{\partial \varphi} &= 0.
\end{aligned}$$

These characteristics are the streamlines, that is their direction is given by: $d\psi = 0$.

2. *Normal characteristics* ($\mathcal{C}_n$) :

$$\begin{aligned}
\xi_3^{(\varphi)} &\quad \text{– may be chosen arbitrarily}, \\
\xi_3^{(\psi)} &= 0, \\
\boldsymbol{\omega}_3^T &= (W^{(4)}, -W^{(3)}, -W^{(2)}, W^{(1)}, 0).
\end{aligned}$$

The compatibility condition is:

$$\frac{1}{C}\frac{\partial C}{\partial \psi} - \frac{1}{\kappa\gamma z S}\frac{\partial S}{\partial \psi} + \frac{2+\gamma z}{2\gamma z D}\frac{\partial D}{\partial \psi} = 0. \tag{29}$$

These characteristics are orthogonal to the streamlines.

3. *Mach lines:* $(\mathcal{C}_\pm)$:

$$\begin{aligned}
\xi_{4,5}^{(\varphi)} &= Cs, \\
\xi_{4,5}^{(\psi)} &= \pm B(\psi)\rho, \\
\boldsymbol{\omega}_{4,5}^{T} &= (s^2F^{(4)} \mp sF^{(3)},\ -s^2F^{(3)} \mp sF^{(4)},\ (1+\gamma z)F^{(2)} \pm sF^{(1)}, \\
&\quad -(1+\gamma z)F^{(1)} \pm sF^{(2)},\ -p\kappa z(2+\gamma z)J_1J_2/(2D)\ ), \\
\text{where} & \\
s &= \sqrt{z-1}.
\end{aligned}$$

This family of characteristic lines only exists when $z > 1$.
Let,

$$D_\pm = sC\frac{\partial}{\partial\varphi} \pm B(\psi)\rho\frac{\partial}{\partial\psi},$$

where $D_\pm$ is the operator of differentiation along $\mathcal{C}_\pm$. The compatibility conditions can then be written as:

$$s\ g(z)D_\pm z \mp D_\pm\theta + \frac{s}{\kappa\gamma zS}D_\pm S - \frac{s}{\gamma zD}D_\pm D = 0.$$

It follows from above that, in the case of a supersonic flow, the governing system (13) is hyperbolic. However, unlike the system of Euler equations in Cartesian coordinates, (13) has characteristics lines $\mathcal{C}_n$, being produced as a result of the introduction of the unknown C.

Remark. In the case of axisymmetric flows, the fluxes in (13) depend not only on U, but on y as well. This makes it necessary to add one more equation to (13):

$$\frac{\partial y}{\partial\varphi} = vJ_2, \tag{30}$$

which follows from (7). The derivation of characteristics and compatibility conditions for the resulting extended system may be done in the same manner as in the case of plane geometry. The equation (30) then becomes one more compatibility condition imposed along $\mathcal{C}_0$.

2.6 Boundary Conditions

In this Section we discuss some problems associated with imposing boundary conditions in the φ – ψ plane. Namely, the boundary conditions for the unknown C are formulated and the ways of applying the impermeability boundary conditions are discussed.

2.6.1 Boundary conditions for the unknown C

The compatibility condition (29), which is valid along the characteristics $\mathcal{C}_n$ (see Fig. 2) shows that C may be specified along $A'B'$. It also follows from (29), that if C is prescribed strictly positive values along this part of the boundary, then it remains strictly positive in $A'B'C'D'$.

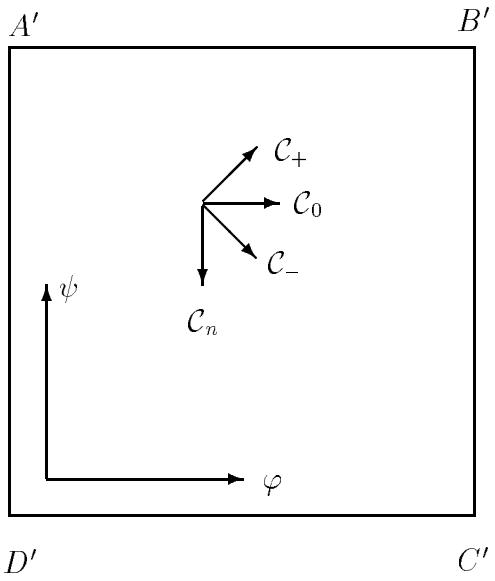

Figure 2: The characteristics directions.

2.6.2 Impermeability boundary conditions

The impermeability boundary conditions must be satisfied by the solution on the rigid walls. Consider, as an example, the part of the boundary $A'B'$, which is an image of the wall AB (see Fig. 1). According to these conditions, in the x–y plane the velocity vector must be tangential to the wall. This means that the velocity vector argument is specified as:

$$\theta \mid_{AB} \;=\; \theta_0(x) \equiv \arctan(\frac{dy}{dx} \mid_{AB}), \tag{31}$$

where the derivative $\frac{dy}{dx}$ along AB is known, because the shape of the wall is given.

To impose the same conditions along $A'B'$ in the $\varphi - \psi$ plane requires to specify θ in terms of φ. However, the dependence between x and φ along the wall is not know beforehand. Several ways to overcome this difficulty are outlined below.

Imposing the boundary conditions iteratively

If the flow under consideration is transonic and some iterative approach is applied to its calculation, one can use the values from the previous iteration to resolve (8). This would give the "updated" boundary conditions to apply on the current iteration. The described procedure should be repeated on each of the following iterations until convergence of the iterative algorithm is achieved.

Choice of proper boundary values of C

In Section 2.6.1 it was established that the values of the unknown C can be specified along $A'B'$. If we choose:

$$C \mid_{A'B'} \;=\; \frac{1}{q \mid_{A'B'}},$$

then, taking into account that $udy - vdx = 0$ along $A'B'$, we obtain:

$$d\varphi \mid_{A'B'} \quad = \quad (1 + (\frac{dy}{dx} \mid_{A'B'})^2)^{\frac{1}{2}} dx \equiv dl,$$

where l is the length of the arc measured along AB.

Consequently, we can choose $\varphi = l$ along AB, and the boundary conditions can be easily transferred from AB to $A'B'$.

Choice of x and y as independent variables

In the case of potential flow, the governing equations reduce to the system of two second order equations with the unknowns x and y (see Section 2.4.2). For this system, it is necessary to impose two boundary conditions along the rigid wall:

$$y = y_0(x),$$
$$\frac{\partial x}{\partial \varphi}\frac{\partial x}{\partial \psi} + \frac{\partial y}{\partial \varphi}\frac{\partial y}{\partial \psi} = 0,$$

where y_0 is a given wall shape function. The first one states that the shape of the wall is specified, and the second ensures orthogonality of the lines $\varphi = const$ to the wall. Note that, as the given formulation uses both x and y as unknowns, it is possible to avoid difficulties associated with the unknown relation between φ and x along the boundary.

Special types of boundary conditions

There are certain classes of problems for which the boundary conditions may be applied without encountering difficulties associated with their mapping from x–y to φ–ψ plane. They are listed below:

1. *Purely supersonic flows*
   In this case the governing equations are hyperbolic, and the solution can be found using marching methods (see Section 3, for example). In any of these methods the solution is calculated in one sweep "from left to right" over the computational domain. In the course of this sweep the relation (8) can be solved to find x as a function of φ along the wall and then the boundary conditions (31) can be imposed on $A'B'$.

2. *Flows with free surfaces*
   Along the free surface, we need to impose the constant pressure or Mach number distribution, while the shape of this part of the boundary is to be found from the solution. As this distribution is constant, it does not require a knowledge of the relation between x and φ.

3. *Homogeneous boundary conditions*
   If a part of the boundary is a straight line (the plane or axis of symmetry, for instance), the boundary conditions become $\theta = const$. As in the previous case, applying this condition does not require the knowledge of $x = x(\varphi)$ along the wall.

4. *Optimal design problems*
   In this case, the shape of the boundary in x–y plane is not specified, but it should be found

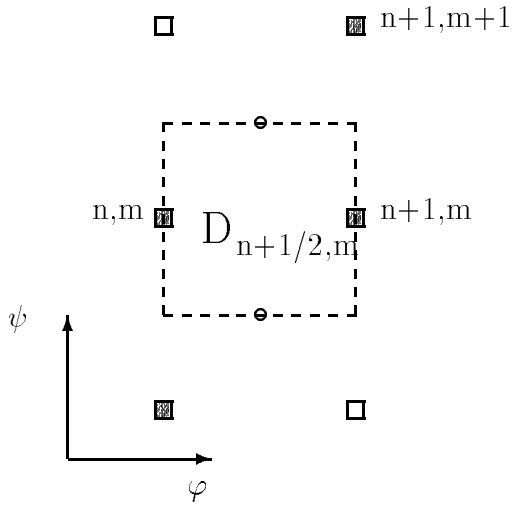

Figure 3: Finite volume and computational stencil.

from the solution procedure. This shape should give the optimal value for some functional (drag or lift, for instance), which is calculated using the contour integral along the wall. This integral may be rewritten in φ–ψ plane, so that the optimal design problem may be reformulated in streamline coordinates.

3 A Conservative Hybrid Grid-characteristics Scheme.

3.1 Conservative approximation of the governing system

Consider purely supersonic flow. In this case the governing system (13) becomes hyperbolic and it may be resolved using a marching scheme.

To construct the difference approximation, consider the finite volume $D_{n+1/2,m}$ shown on Figure 3 with a dashed line. Writing (12) for this volume gives:

$$\oint_{\partial D_{n+1/2,m}} W d\psi - F d\varphi = \nu \int\int_{D_{n+1/2,m}} H d\psi d\varphi$$

Consider the approximation of the above relation on the stencil, which consists of the nodes $(n, m-1)$, (n, m), $(n+1, m)$ and $(n+1, m+1)$ (see Fig. 3):

$$\frac{W_m^{n+1} - W_m^n}{h_\varphi} + \frac{F_{m+1/2}^{n+1/2} - F_{m-1/2}^{n+1/2}}{h_\psi} = \nu H_m^{n+1/2}. \tag{32}$$

As the chosen stencil has two nodes on the upper layer, it is suitable for the approximation of the hyperbolic system (13), which has a family of characteristics $\varphi = const$.

Because the vector of primitive variables U as well as the fluxes W and F are stored at the nodes of the grid, it is necessary to interpolate these values to calculate $F_{m-1/2}^{n+1/2}$ and $F_{m+1/2}^{n+1/2}$. Consider the following interpolation procedure:

$$F_{m+1/2}^{n+1/2} = R_{m+1/2} F_{m+1}^{n+1} + (I - R_{m+1/2}) F_m^n, \tag{33}$$

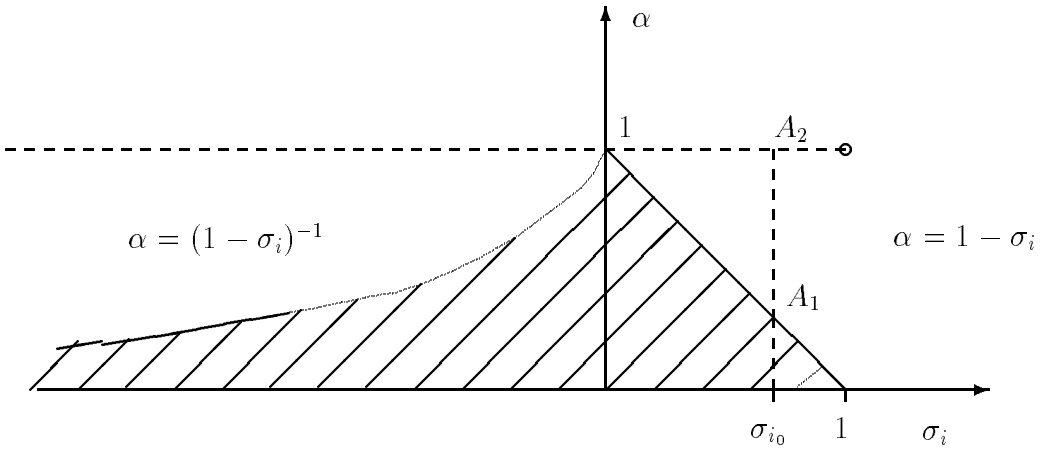

Figure 4:

$$\begin{aligned} F^{n+1/2}_{m-1/2} &= R_{m-1/2}F^{n+1}_m + (I - R_{m-1/2})F^n_{m-1}, \\ H^{n+1/2}_m &= (H^n_m + H^{n+1}_m)/2, \end{aligned} \tag{34}$$

where $R_{m\pm1/2}$ are interpolation matrices. To choose them properly, we consider Riemann invariants and characteristics of the linearized system.

3.2 Linearized system of equations

For a finite volume $D_{n+1/2,m}$, consider the local linearization of the system (13):

$$A_0^{(\varphi)}\frac{\partial U}{\partial \varphi} + A_0^{(\psi)}\frac{\partial U}{\partial \psi} = \nu H_0, \tag{35}$$

where the Jacobian matrices $A_0^{(\varphi)}$ and $A_0^{(\psi)}$ are calculated at the node (n, m). As in Section 2.5 we denote $\xi_i^{(\varphi)}$, $\xi_i^{(\psi)}$ and $\boldsymbol{\omega}_i$ – the eigenvalues and left eigenvectors of the characteristic equation (27).

For the linear system (35) we can introduce the Riemann invariants u_i :

$$u_i = \boldsymbol{\omega}_i^T A_0^{(\varphi)} U.$$

The compatibility condition along the respective characteristic line then becomes a linear advection equation:

$$\xi_i^{(\psi)}\frac{\partial u_i}{\partial \varphi} - \xi_i^{(\varphi)}\frac{\partial u_i}{\partial \psi} = r_i,$$

where

$$r_i = \boldsymbol{\omega}_i^T H_0.$$

For the four–node stencil in consideration there exists a one–parameter family of finite difference equations, approximating the above advection equation [45]:

$$(2-\sigma_i)(u_i)_m^{n+1} - \alpha(2-\sigma_i)(u_i)_m^n - (1-\alpha(1-\sigma_i))(u_i)_{m-1}^n \\ -(1-\sigma_i-\alpha)(u_i)_{m+1}^{n+1} - (r_i)_m^n = 0, \tag{36}$$

where,

$$\sigma_i \;=\; -\frac{h_\varphi \xi_i^{(\varphi)}}{h_\psi \xi_i^{(\psi)}} - \text{a CFL number.}$$

Each value of the parameter α gives a scheme which approximates the advection equation with at least first order accuracy. Consider Fig. 4. One can prove the following:

1. The dashed line $\alpha = 1$ corresponds to the schemes with at least second order accuracy;
2. Shaded area corresponds to the schemes with "positive approximation" [45], that is, the schemes with positive coefficients. This is sufficient for their monotonicity;
3. The coefficient of the effective viscosity, generated by the scheme, is proportional to the distance between the point corresponding to this scheme on the diagram on Fig. 4, and the dashed line $\alpha = 1$;
4. The stability condition for this family of approximations is $\sigma_i < 1$.

Therefore, for a given value of $\sigma_i = \sigma_{i_0} < 1$, we have the second order scheme A_2 (which is not monotone, unless $\sigma_{i_0} = 0$), as well as the first order monotone scheme A_1 located on the boundary of the shaded area (see Fig. 4). It follows from above, that, for a given value of σ_{i_0}, the scheme A_1 has the minimal coefficient of the effective viscosity among all monotone schemes. Hence, the scheme A_1 possesses minimal smearing properties among those monotone schemes. The family of schemes which is of interest for us is then represented by the chord A_1A_2. One can choose a scheme from this family closer to A_2 to obtain better resolution at the price of possible non–monotonicity. In a similar way, a shift towards A_1 results in the damping of oscillations at the price of lesser local accuracy.

To apply this result to the linearized system (35) rewrite (32) as:

$$\frac{(W_0)_m^{n+1} - (W_0)_m^n}{h_\varphi} + \frac{(F_0)_{m+1/2}^{n+1/2} - (F_0)_{m-1/2}^{n+1/2}}{h_\psi} = \nu (H_0)_m^{n+1/2}. \tag{37}$$

where,

$$W_0 \;=\; A_0^{(\varphi)} U, \\ F_0 \;=\; A_0^{(\psi)} U.$$

To calculate the fluxes $(F_0)_{m\pm1/2}^{n+1/2}$ we again resort to the interpolation procedure (33) and (34). However, as we consider the linear equation, we can put $R_{m-1/2} = R_{m+1/2} \equiv R$, where R is a square matrix with constant entries.

Choose this matrix to be:

$$R \;=\; \Omega^{-1}\tilde{R}\,\Omega \tag{38}$$

where Ω is a matrix composed of the rows $\boldsymbol{\omega}_i^T$, and $\tilde{R}$ is a diagonal matrix with diagonal entries $\tilde{R}_{ii}$.

Multiplying (37) by $\boldsymbol{\omega}_i^T$, one can obtain:

$$\begin{aligned}(1-\sigma_i\tilde{R}_{ii})(u_i)_m^{n+1} - (1-\sigma_i+\sigma_i\tilde{R}_{ii})(u_i)_m^n - (\sigma_i-\sigma_i\tilde{R}_{ii})(u_i)_{m-1}^n \\ +\sigma_i\tilde{R}_{ii}(u_i)_{m+1}^{n+1} - \nu(1-\sigma_i\tilde{R}_{ii})h_\varphi h_\psi r_m^n = 0,\end{aligned} \tag{39}$$

Comparison between the expressions (36) and (39) gives the link between the value of $\tilde{R}_{ii}$ and the parameter α from (36):

$$\tilde{R}_{ii} \;=\; \frac{\sigma_i+\alpha-1}{(1+\alpha)\sigma_i}.$$

It follows from this relation and Fig. 4 that setting

$$\tilde{R}_{ii} = \frac{1}{2}$$

will result in the second order approximation, while,

$$\tilde{R}_{ii} = \frac{1}{2} - \frac{\mathrm{Sgn}(\sigma_i)}{2}$$

gives the first order monotone scheme with minimal effective viscosity coefficient.

To obtain the *hybrid scheme* [45] we should set

$$\tilde{R}_{ii} = \frac{1}{2} - \beta\frac{\mathrm{Sgn}(\sigma_i)}{2}, \tag{40}$$

where $0 \le \beta \le 1$ – the parameter. In accordance with what has been mentioned above, the parameter β should be chosen close to zero in the regions where the solution is smooth enough and close to 1 in the regions where the solution has large gradients (ie near shocks). In this work we use the algorithm for choosing the values of β in accordance with the local behaviour of the solution which is given in [45].

3.3 Generalization to the nonlinear case

To generalise the idea of hybrid scheme to the nonlinear case, choose the matrices $R_{m\pm1/2}$ in (33) and (34) in accordance with (38). Then, (32), which gives the approximation for the finite volume $D_m^{n+1/2}$, can be rewritten as:

$$W_m^{n+1} - \frac{h_\varphi}{h_\psi}\Omega_{m-1/2}^{-1}\tilde{R}_{m-1/2}\Omega_{m-1/2}F_m^{n+1} =$$
$$\nu h_\varphi H_m^{n+1/2} + W_m^n - \frac{h_\varphi}{h_\psi}(F_m^n - F_{m-1}^n)$$
$$-\frac{h_\varphi}{h_\psi}\Omega_{m+1/2}^{-1}\tilde{R}_{m+1/2}\Omega_{m+1/2}(F_{m+1}^{n+1} - F_m^n)$$
$$-\frac{h_\varphi}{h_\psi}\Omega_{m-1/2}^{-1}\tilde{R}_{m-1/2}\Omega_{m-1/2}F_{m-1}^n.$$

At the current step of the computational algorithm, the right–hand side is known from the previous step. The left–hand side is then solved by Newton iterative technique with respect to U_m^{n+1}. At the next step, the same procedure is repeated for the equation corresponding to the finite volume $D_{m-1}^{n+1/2}$ to find U_{m-1}^{n+1}.

It should be noted that, although the governing system has a family of characteristic lines $\varphi = const$, normal to streamlines, the stable solution process can be implemented by marching in the direction of streamlines. This is due to the fact that the computational stencil has two nodes on the upper layer, ie the scheme is implicit. At the same time, as there are only two nodes on the upper level, the resulting solution procedure does not require global iterations in order to find the values of U^{n+1}

4 An Iterative Algorithm for a Second Order Full–Potential Equivalent Equation.

In the case of transonic potential flow with constant entropy and full enthalpy the function C from (13) can be set equal to any positive function of φ and then the governing system can be reduced to just one second order partial differential equation of a mixed type (see Section 2.4.1 for details):

$$\frac{\partial}{\partial\varphi}\Big(f\frac{\partial y}{\partial\varphi}\Big) + \frac{\partial}{\partial\psi}\Big(\frac{1}{f}\frac{\partial y}{\partial\psi}\Big) = 0,$$

where,

$$\begin{aligned} f &= \frac{J_1}{J_2} = \frac{C(\varphi)}{B(\psi)y^\nu\rho}, \\ \rho &= \rho(z). \end{aligned}$$

The second order equation for y may be considered as the equivalent to the full–potential equation. Then, the difference approximation and the numerical algorithms developed for the full–potential equation may be applied in this case.

The approximating system of finite difference equations is obtained using central difference approximation formulae and the concept of artificial compressibility in supersonic regions:

$$\Delta_\varphi^+ \tilde{f} \Delta_\varphi^- y + \Delta_\psi^+ \frac{1}{f} \Delta_\psi^- y = 0, \tag{41}$$

where

$$\begin{aligned} \tilde{f}_{ij} &= \mu_{ij} f_{ij} + (1 - \mu_{ij}) f_{ij-1}, \\ \mu_{ij} &= \min(1, \max(0, \eta(M^2 - 1))), \\ \eta &> 0 - \text{a parameter.} \end{aligned}$$

To resolve the system of equations (41) the approximate factorization iterative technique was applied:

$$(1 - \tau \Delta_\varphi^+ \tilde{f}^{(n)})(\Delta_\varphi^- - \tau \Delta_\psi^+ \frac{1}{f^{(n)}} \Delta_\psi^-) \varepsilon^{(n)} = \tau \omega R(y^{(n)}), \tag{42}$$

where

$\varepsilon^{(n)}$	$=$	$y^{(n+1)} - y^{(n)}$	– the correction vector,
$R(y^{(n)})$			– the residual vector of the equation (41)
τ, ω			– the iterative parameters.

The operator on the left-hand side of (42) may be inverted in two sweeps over the computational domain. This kind of approximate factorization has been successfully applied earlier to the solution of the velocity vector potential equation in [46].

It was established in Section 2.4.1, that the parameters of the flow z and θ are given implicitly as functions of the unknown function y and its derivatives by the following relations:

$$\begin{aligned} \frac{u}{\rho q^2} &= B(\psi) y^\nu \frac{\partial y}{\partial \psi}, \\ \frac{v}{q^2} &= C(\varphi) \frac{\partial y}{\partial \varphi}. \end{aligned}$$

But in the transonic range, the difficulty of the non–uniqueness of the solution of the above system exists (see Section 2.4.1). In order to overcome this difficulty, instead of solving the system of algebraic relations (20) and (21) we solve the following partial differential equation for the unknown z in transonic regions [41] :

$$\frac{\partial}{\partial \varphi}\Big((1 - z) b \frac{\partial z}{\partial \varphi}\Big) + \frac{\partial}{\partial \psi}\Big(a \frac{\partial z}{\partial \psi}\Big) = -\frac{\partial c}{\partial \varphi}$$

where

$$a = \frac{g(z)}{f} \ , \ b = f g(z),$$

$$c = \nu \frac{v}{y^2 \rho q^2 B(\psi)} \ , \ g(z) = \frac{d}{dz} \ln q.$$

This equation is solved only along those grid lines $\varphi = const$, which have supersonic points. Following [42], we calculate the coefficients of the above equation from the previous iteration, and then apply the SOR iterative algorithm to the resulting system of linear equations.

5 An Iterative Algorithm for the System of Two Equations.

In this Section we consider an iterative algorithm, based upon the formulation of the governing system in the potential flow case which has been developed in Section 2.4.2. Note here that a disadvantage of the formulation proposed in the previous Section is that it is necessary to apply the additional equation for the unknown z in transonic regions. Unlike the second order equation for y, the equation for the unknown z does not express conservation of any physical quantity (such as mass, momentum or energy). Therefore, this equation can not be applied in the vicinity of the discontinuities in the flow.

In Section 2.4.2 the governing system was reduced to the system of two equations:

$$\frac{\partial W^{(p)}}{\partial \varphi} + \frac{\partial F^{(p)}}{\partial \psi} = 0,$$

where fluxes $W^{(p)}$ and $F^{(p)}$ are expressed in terms of derivatives of x and y:

$$W^{(p)} = \begin{bmatrix} f\frac{\partial x}{\partial \varphi} \\ f\frac{\partial y}{\partial \varphi} \end{bmatrix}, \quad F^{(p)} = \begin{bmatrix} \frac{1}{f}\frac{\partial x}{\partial \psi} \\ \frac{1}{f}\frac{\partial y}{\partial \psi} \end{bmatrix}.$$

It was established in Section 2.4.2, that if the unknowns x and y are known as functions of φ and ψ, then the parameters of the flow z and θ can be found in a unique way by solving the algebraic equations (24) and (25).

The approximation of (19) is performed using central differences and artificial compressibility:

$$(W^{(p)}_{i,j+1/2} - W^{(p)}_{i,j-1/2})/h_\varphi + (F^{(p)}_{i+1/2,j} - F^{(p)}_{i-1/2,j})/h_\psi = 0, \tag{43}$$

where,

$$W^{(p)}_{ij+1/2} = \begin{bmatrix} \tilde{f}_{ij+1/2}\frac{x_{ij+1}-x_{ij}}{h_\varphi} \\ \tilde{f}_{ij+1/2}\frac{y_{ij+1}-y_{ij}}{h_\varphi} \end{bmatrix}, \quad F^{(p)}_{i+1/2,j} = \begin{bmatrix} \frac{1}{f_{i+1/2j}}\frac{x_{i+1j}-x_{ij}}{h_\psi} \\ \frac{1}{f_{i+1/2j}}\frac{y_{i+1j}-y_{ij}}{h_\psi} \end{bmatrix},$$

and,

$$\begin{aligned} \tilde{f}_{ij+1/2} &= \frac{C(\varphi)}{B(\psi)y^{\nu}_{ij+1/2}\tilde{\rho}_{ij+1/2}}, \\ \tilde{\rho}_{ij+1/2} &= \rho_{ij+1/2} + \mu_{ij+1/2}(\rho_{ij-1/2} - \rho_{ij+1/2}), \\ \mu_{ij+1/2} &= \max(0, 1 - \frac{1}{M^2_{ij+1/2}}). \end{aligned}$$

To resolve the system (43) the following iterative procedure is applied. First, using the values of x and y from previous iteration, the system (24) and (25) is solved by Newton iterations to find z and θ. The new values of z are used to update the values of the coefficient f. Substituting these values into (43) gives the linearized system for x and y.

The resulting system of linear equations is solved by point Gauss–Seidel method based upon the natural ordering of the unknowns.

The convergence of iterations is accelerated by employing two-level multigrid cycles. The description of the multigrid procedure used in the calculations follows.

Consider a pair of rectangular uniform grids in the $\varphi - \psi$ plane. The first grid is referred to as *a fine grid*. The step sizes in φ and ψ directions for this grid are h_φ and h_ψ. The second grid, *a coarse grid*, is generated by skipping alternate nodes within the fine grid. Similar to the first grid, H_φ, H_ψ denote step sizes in φ and ψ directions for the coarse grid.

Define operators of restriction R_h^H and prolongation P_H^h to be used to pass the information between the grids. Namely, the restriction operator R_h^H acts on a grid function defined on a fine grid and produces a restriction of this grid function on a coarse grid. In this work, this restriction is accomplished by ignoring the values of the grid function at those nodes of the fine grid which do not correspond to nodes of the coarse grid. The prolongation operator P_H^h interpolates the data from the coarse grid to the fine grid. In this work, linear interpolation is used for this purpose.

Denote the residual vector of the system of difference equations (43) computed on the fine grid by N_h. Also, denote the solution vector composed of the values of x and y at the grid nodes of the fine grid by x_h.

The multigrid algorithm used in this work can then be described as follows:

1. Using an initial guess on a fine grid, or data from a previous multigrid cycle, perform k_h point Gauss–Seidel (PGS) iterations for the linearized system of difference equations (43):

$$G_h e_h^{(n)} = N_h^{(n)},$$
$$x_h^{(n+1)} = x_h^{(n)} + e_h^{(n)},$$

   where G_h is an iteration matrix corresponding to the PGS method, $e_h^{(n)}$ is a correction vector, superscripts serve to distinguish the quantities referring to the previous and the next iteration, while subscripts show that all the above quantities are calculated on the fine grid. After each iteration the coefficient f needs to be evaluated to obtain an updated linearization.

2. Perform k_H Gauss–Seidel iterations on the coarse grid as described below.

   2.1 Using the residual on the fine grid, which is known either from step 1, or from the previous iteration on the coarse grid, compute the correction vector for the coarse grid $e_H^{(n)}$:

$$G_H e_H^{(n)} = R_h^H N_h^{(n)}.$$

   2.2 Update the solution on the fine grid, using $e_H^{(n)}$ and the prolongation operator P_H^h:

$$x_h^{(n+1)} = x_h^{(n)} + P_H^h e_H^{(n)}$$

   2.3 Using $x_h^{(n+1)}$, compute $R_h^H N_h^{(n+1)}$. Notice, that for the choice of restriction operator used in this work, this stage requires simply to calculate the residual at alternate nodes of the fine grid.

   2.4 Go to the step 2.1.

3. Go to the step 1.

Interpolating between the grids in a described way allows damping of both the high– and low–frequency components of the error in a more efficient way than on a single grid. Also, typically it is possible to carry the iterations mostly on the coarse grid, where the low-frequency components of the error can be removed using fewer arithmetic operations. Switching to the fine grid could be done periodically when the high–frequency components become dominant.

6 Numerical Results.

In this section results are presented for a series of supersonic and transonic flows calculated using methods which have been described above.

To demonstrate the properties of the hybrid scheme the standard test problem of a supersonic flow ($M_\infty = 2.0$) over the wedge ($\delta = 15°$) was solved using the scheme described in Section 3. Fig. 5 shows Mach number plotted against the coordinate ψ directed across the flow. These calculations were performed using first order monotone ($\beta = 1$ in (40)), second order ($\beta = 0$) and hybrid schemes. In the case of the hybrid scheme the values of the parameter β at each node were chosen depending on the local behaviour of the solution as described in [45]. The comparison between these solutions shows that the first order monotone scheme smears the shock over $5 - 7$ nodes; the second order scheme gives width of the shock equal to $3 - 4$ nodes but also produces non-physical oscillations in the solution. The solution given by the hybrid scheme has the shock width of $4 - 5$ nodes and it remains monotone.

Fig. 6 shows the pressure and entropy function contours as well as the streamline computational grid in the supersonic part of the nozzle and in the jet emerging from it. This flow was computed using the hybrid scheme given in Section 3.

In Fig. 7 and Fig. 8, application of the iterative technique outlined in Section 4 is illustrated for the calculation of the transonic potential gas flow in a converging–diverging nozzle, which has earlier been studied experimentally in [47]. The comparison of the computed pressure and Mach number distribution along the wall with the experimental data shows good agreement except in the region downstream of the nozzle throat. This loss of accuracy may be ascribed to the presence of the shock in this region resulting in non–zero vorticity in real flow and hence inappropriateness of the potential flow model.

Finally, Fig. 9 and Fig. 10 show the results obtained using the formulation and the iterative algorithm described in Section 5. The subsonic flow through a bumpy axisymmetric channel was calculated. Fig. 9 demonstrates the influence of the number of iterations at each grid level in the two–grid cycle on the convergence rate, and Fig. 10 shows the solution.

7 Acknowledgements.

The author would like to thank Dr. R.M.Barron, Department of Mathematics and Statistics and Fluid Dynamics Research Institute, University of Windsor and Dr. I.J.Sobey, Oxford University Computing Laboratory (OUCL) for their help and guidance.

The work reported here was supported by a visiting graduate scholarship at OUCL provided by Soros Foundation, New York. Also, this research was supported in part by the Institute for Mathematics and Its Applications, University of Minnesota with funds provided by the National Science Foundation.

References

[1] Von Mises, R. *Bemerkungen zur Hydrodynamik.* ZAMM, Vol. 7, p. 425, 1927.

[2] Stanitz, J.D. *Design of two-dimensional channels with prescribed velocity distributions along the channel walls, Part I – Relaxation solutions.* NACA TN 2595 (1952).

[3] Stanitz, J.D. *Design of two-dimensional channels with prescribed velocity distributions along the channel walls, Part II – Solution by Green's function.* NACA TN 2595 (1952).

[4] Martin, M.H. *A new approach to problems in two dimensional flow.* Quart. J. Appl. Math., Vol. VIII, No.2, pp.137–150, 1950.

[5] Martin, M.H. *The flow of a viscous fluid.I* Archives for Rational Mechanics and Analysis, Vol. 41, pp. 266–286, 1971.

[6] Barron, R.M., An, C.-F. and Zhang, S. *Survey of the streamfunction-as-a-coordinate method in CFD.* Proc. of the Inaugural Conference of the CFD Society of Canada, Montreal, Canada, June 14–15, 1993, pp.325–336.

[7] Greywall, M.S. *Streamwise computation of 2–D incompressible potential flows.* J. Comp. Phys., Vol. 59, pp. 224–231, 1985.

[8] Barron, R.M. *Computation of incompressible potential flow using von Mises coordinates.* Mathematics and Computers in Simulation, Vol. 31, pp. 177–188, 1989.

[9] Naeem, R.K. and Barron, R.M. *Lifting airfoil calculations using von Mises variables.* Comm. Appl. Num. Methods, Vol. 5, pp. 203–210.

[10] Barron, R.M., Zhang, S., Chandna, A. and Rudraiah, N. *Axisymmetric potential flow calculations. Part 1: Analysis mode.* Comm. Appl. Num. Methods, Vol 6, pp. 437–445, 1990.

[11] Barron, R.M. and Naeem, R.K. *Numerical solution of transonic flows on a streamfunction co-ordinate system.* Intl. J. Num. Methods in Fluids, Vol. 9, pp. 1183–1193, 1989.

[12] Naeem, R.K. and Barron, R.M. *Transonic computations on a natural grid.* AIAA J., Vol. 28, pp. 1836–1838, 1990.

[13] Barron, R.M. and Naeem, R.K. *2-D transonic calculations on a flow-based grid system.* Mathematics and Computers in Simulation, Vol. 33, pp. 65-67, 1991.

[14] An, C.-F. and Barron, R.M. *Numerical solution of transonic full-potential-equivalent equations in von Mises coordinates.* Intl. J. Num. Methods in Fluids, Vol. 15, pp. 925–952, 1992.

[15] Barron, R.M. *A non-iterative technique for design of airfoils in incompressible potential flow.* Comm. Appl. Num. Methods, Vol. 6, pp. 557–564, 1990.

[16] Barron, R.M. and An, C.-F. *Analysis and design of transonic airfoils using streamline coordinates.* Proc. 3rd Intl. Conf. on Inverse Design Concepts and Optimization in Eng. Sci., Washington, DC, USA, ed. by G.S.Dulikravich, pp. 359–370, 1991.

[17] Zhang, S., Barron, R.M. and Rudraiah, N. *Axisymmetric potential flow calculations. Part 2: Design mode.* Comm. Appl. Num. Methods, Vol. 7, pp. 563–567, 1991.

[18] Barron, R.M. and Hamdan, M.N. *Brinkman and Forchheimer corrections to Darcy's Law: Applications to flow over curved boundaries.* Proc. Canadian Applied Math. Society, 11 Annual Conf., Halifax, Nova Scotia, pp. 453–462, May 1990.

[19] Hamdan, M.N. and Barron, R.M. *Applications of von Mises coordinates in porous media flow.* J. Comput. Applied Math., Vol. 39, pp.353–361, 1992.

[20] Barron, R.M. and Hamdan, M.N. *The double von Mises transformation in the study of two-phase fluid flow over curved boundaries: Theory and analysis.* Intl. J. Num. Methods in Fluids, Vol. 14, pp.883–905, 1992

[21] Hui, W.H. and Loh, C.Y. *A new Lagrangian method for steady supersonic flow computation. Part I. Godunov scheme.* J. Comput. Phys., Vol. 89, pp. 207–240, 1990.

[22] Loh, C.Y. and Liou, M.S. *A new Lagrangian method for solving 3-D steady supersonic flow problems.* Proc. 1st European CFD Conference, Brussels, Belgium, Sept. 7–11, 1992.

[23] Loh, C.Y. and Liou, M.S. *Computing 3–D steady supersonic flow via a new Lagrangian approach.* AIAA Paper 93-0891 (1993).

[24] Stanitz, J.D. *General design method for three-dimensional potential flow fields. Part I – Theory.* NASA CR 3288 (1980).

[25] Stanitz, J.D. *General design method for three-dimensional potential flow fields. Part II – Computer program DIN3D1 for simple, unbranched ducts.* NASA CR 3926 (1985).

[26] Pearson, C.E. *Use of streamline coordinates in the numerical solution of compressible flow problems.* J. Comp. Phys., Vol. 42, pp. 257–265, 1981.

[27] Owen, D.R. and Pearson, C.E. *Numerical solution of a class of steady–state Euler equations by a modified streamline method.* AIAA 88-0625, 1988.

[28] Huang, C.-Y. and Dulikravich, G.S. *Stream function and stream function coordinate (SFC) formulation for inviscid flow field calculations.* Computer Methods Appl. Mech. Eng., Vol. 59, pp. 155–177, 1986.

[29] Dulikravich, G.S. *A stream-function-coordinate (SFC) concept in aerodynamic shape design.* AGARD-R-780, Brussels, Belgium, pp. 6.1–6.6, 1990.

[30] Honda, M., *Stream-function coordinates in rotational flow and an analysis of the flow in a shock layer. Part I: Two- dimensional flow.* J. Inst. Maths. Applics., Vol. 1, pp. 127–148, 1965.

[31] Honda, M., *Stream-function coordinates in rotational flow and an analysis of the flow in a shock layer. Part II: Axisymmetric flow.* J. Inst. Maths. Applics., Vol. 2, pp. 55–75, 1966.

[32] Takahashi, K. and Tsukiji, T. *Numerical analysis of a laminar jet using a streamline coordinate system.* Transactions of the CSME, Vol. 9, pp. 165–170, 1985.

[33] Tsukiji, T. and Takahashi, K. *Numerical analysis of an axisymmetric jet using a streamline coordinate system.* JSME Intl. J., Vol. 30, pp. 1406–1413, 1987.

[34] Zarbi, G. and Takahashi, K. *Prediction of the laminar two-dimensional jet flow through a convergent channel.* JSME Intl. J., Series II, Vol. 24, pp. 115–121, 1991.

[35] Finnigan, J.J. *A streamline coordinate system for distorted two-dimensional shear flows.* J. Fluid Mech., Vol. 130, pp.241-258, 1983.

[36] Finnigan, J.J. and Bradley, E.F. *The turbulent kinetic energy budget behind a porous barrier: An analysis in streamline co-ordinates.* J. Wind Eng. and Ind. Aerodyn., Vol. 15, pp. 157-168, 1983.

[37] Finnigan, J.J. *Streamline Coordinates, Moving Frames, Chaos and Integrability in Fluid Flow. In* Topological Fluid Mechanics. (Cambridge, 1989) pp. 64–74, Cambridge University Press, Cambridge, 1990.

[38] Karataev, S.G. *A numerical method for calculation of viscous flows in channels.* Communications in Applied Mathematics, USSR Academy of Science Computing Center, Moscow, pp. 3–34, 1989, (in Russian).

[39] Latypov, A.M. *On a form of equation for two-dimensional stationary flows of compressible gas.* Proc. XIV Conf. of Young Scientists, MFTI, VINITI 11.09.89, No.5761-V89, pp. 77–81, 1989, (in Russian).

[40] Latypov, A.M. *On application of natural independent variables to the steady-state Euler equations formulation.* Proc. XV Conf. of Young Scientists, MFTI, VINITI, No. 6174-V90, pp. 79–82, 1990, (in Russian).

[41] Latypov, A.M. and Shipilin,A.V. *On an iterational method for calculating sub- and transonic internal flows.* Computational Mathematics and Mathematical Physics, Vol. 31, No. 5, pp. 92-99, 1991. [2]

[42] Osipov, I.L., Shipilin, A.V. and Shulishnina, N.P. *A numerical method for calculation of gas flows in channels and nozzles in direct, inverse and combined modes.* Zh. Vychisl. Mat. i Mat. Fiz., Vol. 27, No.10, pp.1563–1572, 1987, (in Russian).

[43] Osipov, I.L., Pashchenko V.P. and Shipilin, A.V. *Computation of inviscid gas flows in ducts with sharply varying geometry.* USSR Comp. Math. and Math. Phys., Vol. 18, No.4, pp.143–152, 1978.

[44] Ovsyannikov, L.V. *Lectures on Fundamentals of Gas Dynamics* Nauka, Moscow, 1981 (in Russian).

[45] Magomedov,K.M. and Holodov,A.S. *The Grid-Characteristics Numerical Methods.* Nauka, Moscow, 1988 (in Russian).

[46] Ivanov,M.Ya. and Koretskii V.V. *Calculation of flows in two and three dimensional nozzles by the approximate factorization method.* USSR Computational Mathematics and Mathematical Physics, Vol. 25, No. 5, pp. 56-67, 1985.

[47] Cuffel,R.F., Back,L.H. and Massier, P.F. *Transonic flowfield in a supersonic nozzle with small throat radius of curvature.* AIAA J., Vol.7, No. 7, pp. 1364-1366, 1969.

[2] The original Russian version of this paper has appeared in Zh. Vychisl. Mat. i Mat. Fiz., 31, 5, 767-776, 1991

Figure 5: Mach number vs psi coordinate.

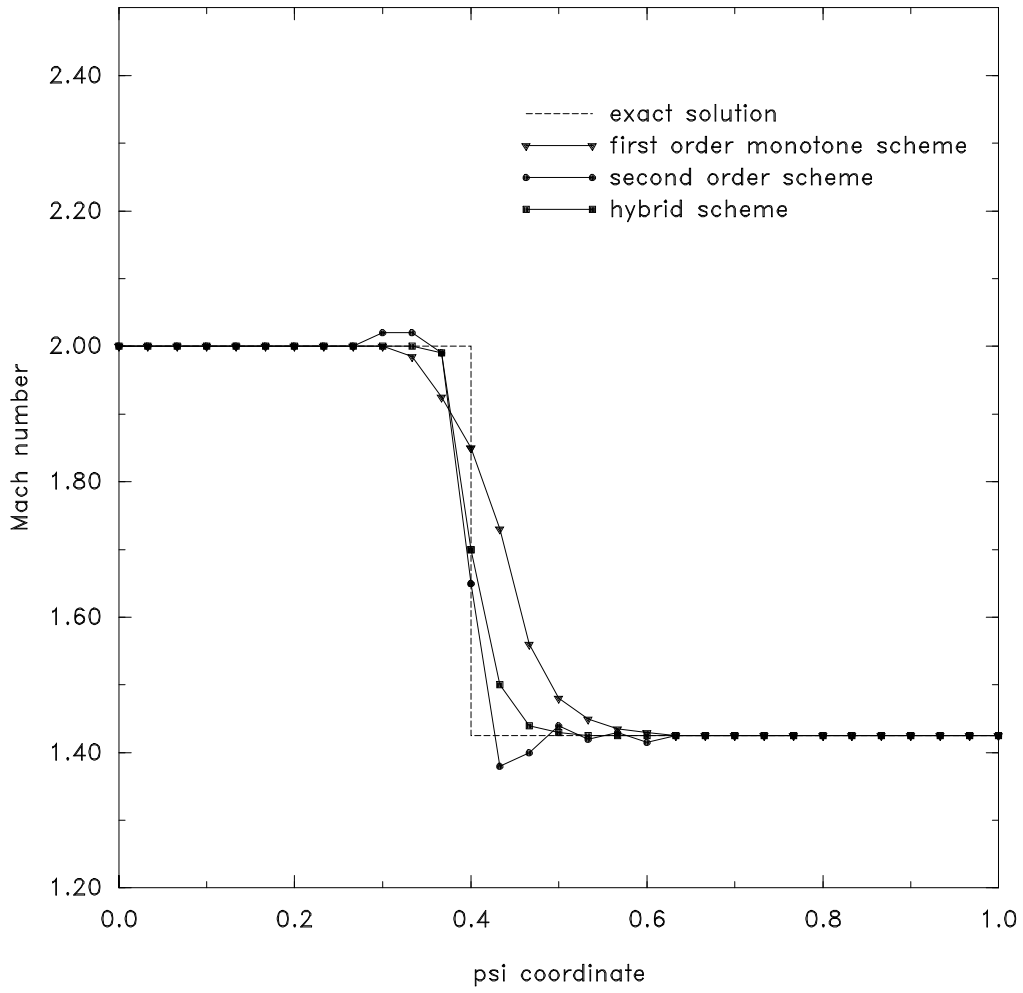

Figure 6: A supersonic nozzle and the jet emerging from it.

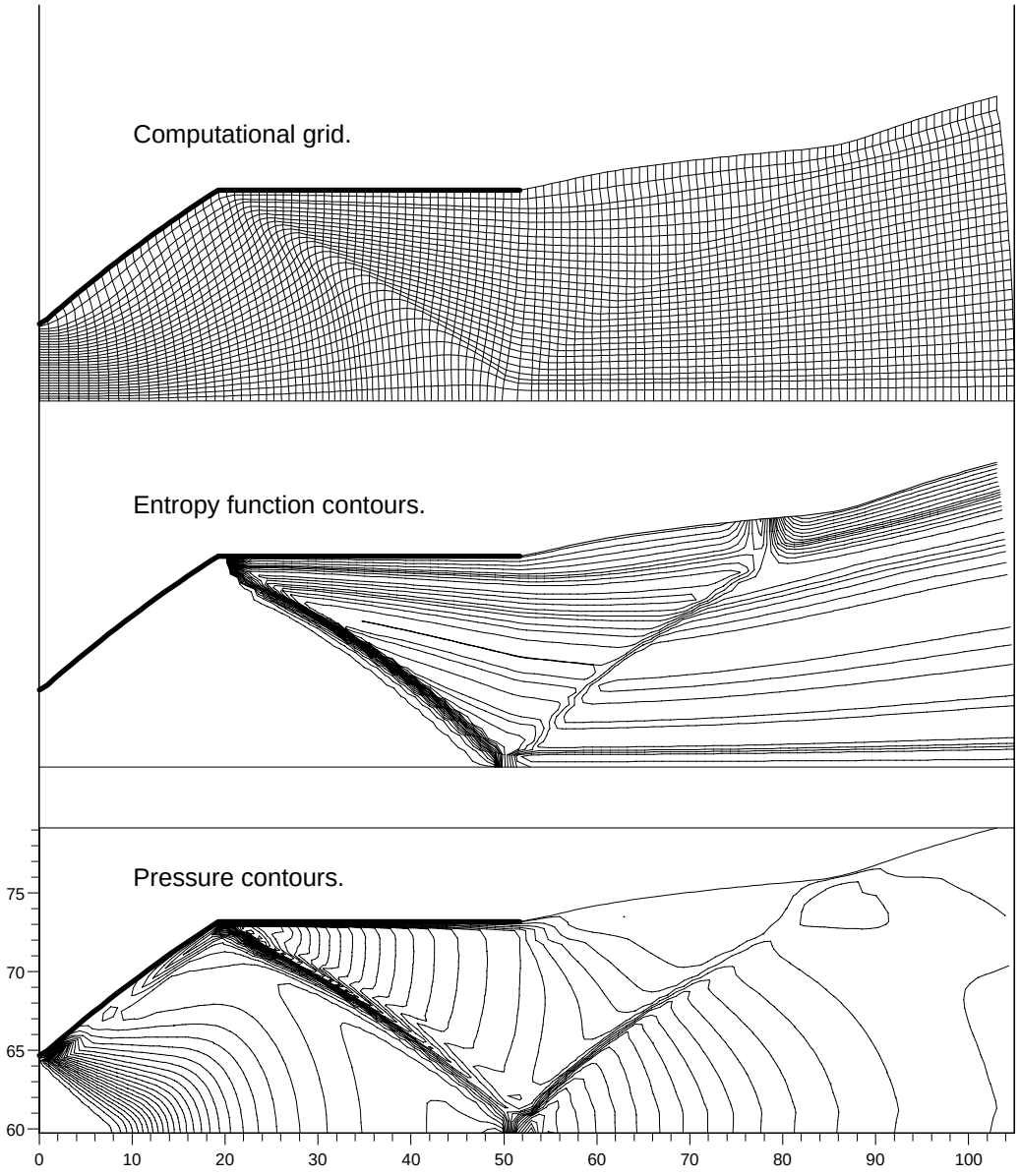

Figure 7: A transonic flow in a nozzle.

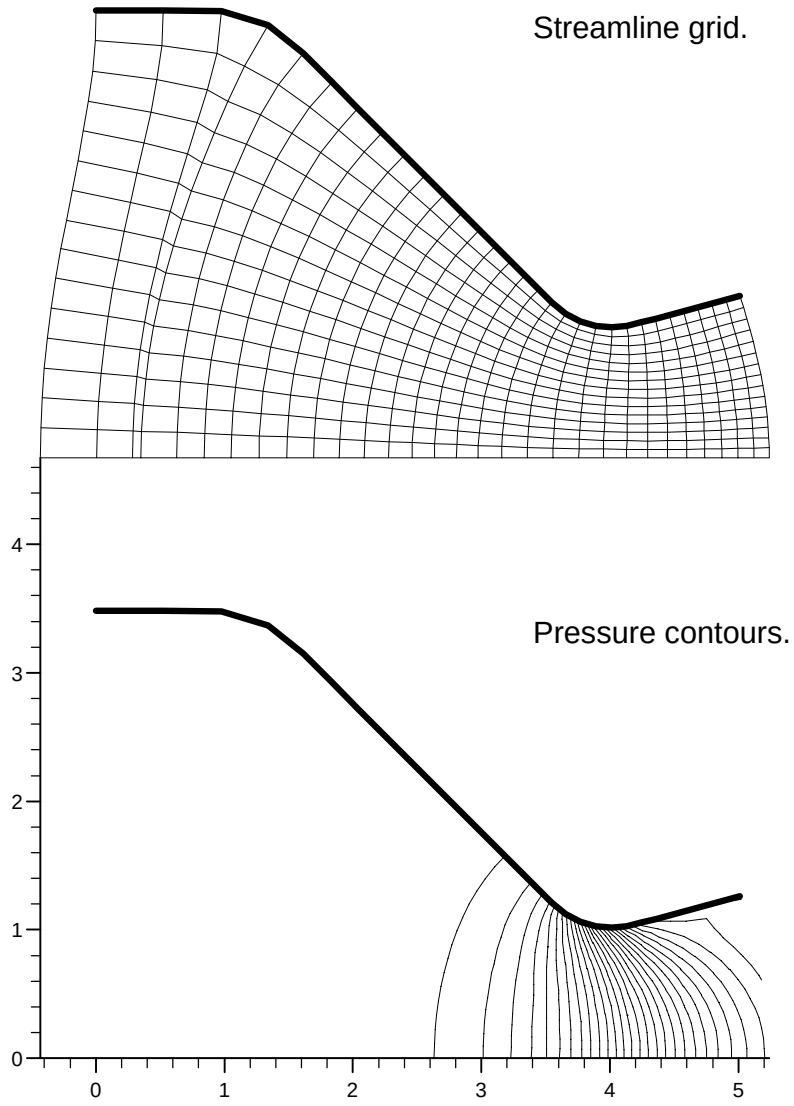

Figure 8: Pressure and Mach number distributions along the wall.

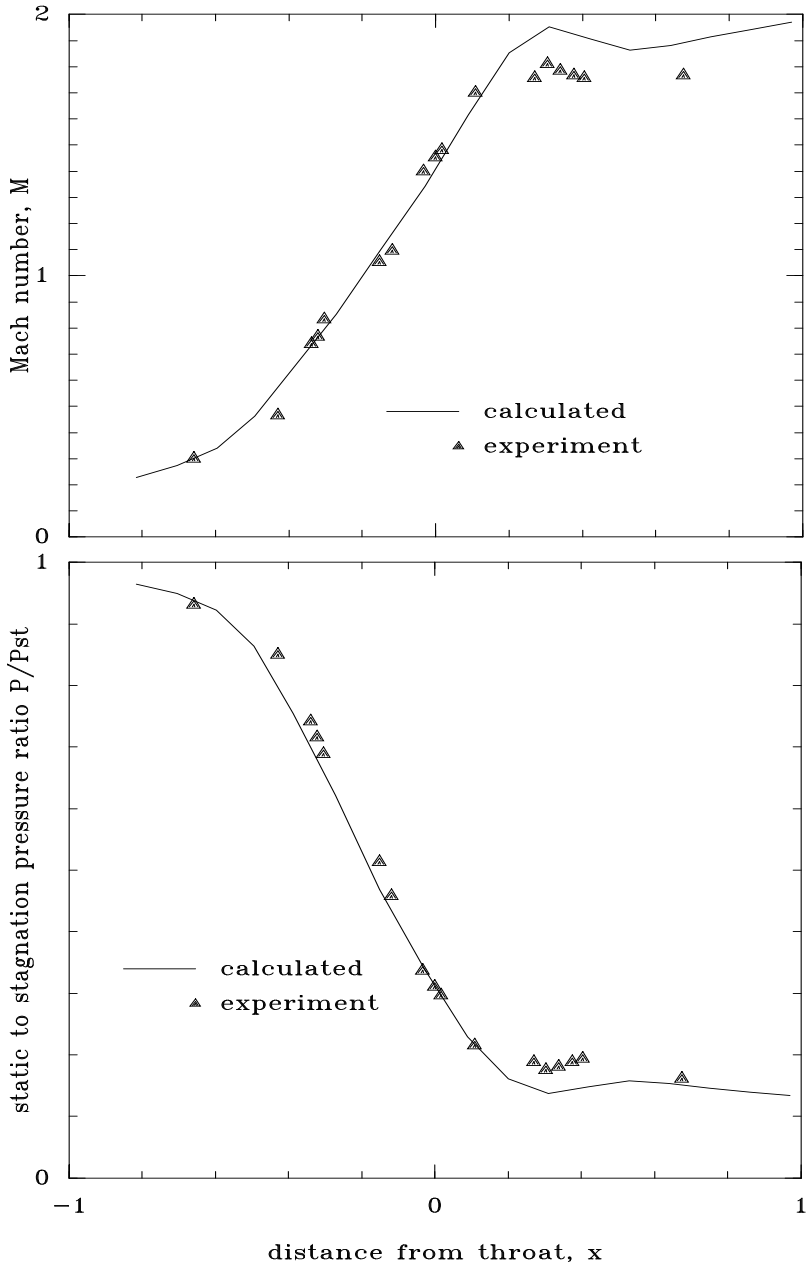

Figure 9: The influence of the number of iterations on each grid level on the convergence rate.

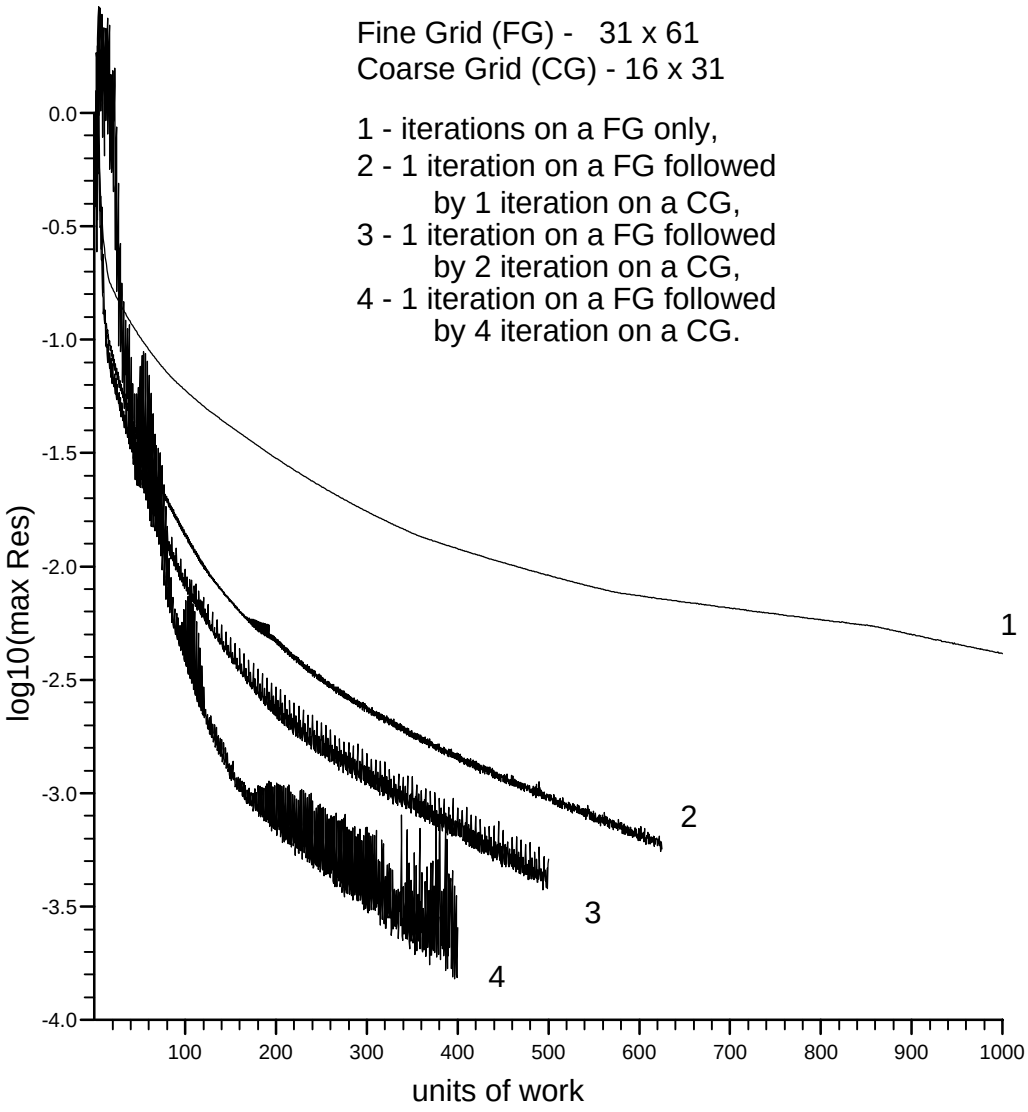

Figure 10: Subsonic flowfield in the axisymmetric bumpy channel.